








Fast Frequency Support Through LED Street Lighting in Small Non-Synchronous Power Systems

Sergio Bruno , *Member, IEEE*, Giovanni Giannoccaro , Cosimo Iurlaro , *Graduate Student Member, IEEE*, Massimo La Scala , *Fellow, IEEE*, Marco Menga , *Member, IEEE*, Carmine Rodio , *Graduate Student Member, IEEE*, and Roberto Sbrizzai 

Abstract—Small-sized non-synchronous islands, which are inherently characterized by low system inertia, will face in the next years the challenge of integrating larger and larger amount of renewable energy sources, leading to further reduction of inertia. Several means to support inertia and frequency transients have been proposed in the literature, including energy storage systems, distributed generation, and demand response. LED street lighting systems are widespread control resources, which in a smart grid scenario, can be regulated by means of local or remote control signals. This article investigates the possibility to regulate the power consumption of LED street lighting to provide frequency support in a system characterized by reduced total inertia. Tests are carried out integrating the simulation of the non-synchronous power system of an Italian small island with the response of an actual LED street lamp, in a Power Hardware-in-the-Loop testing environment. Both synthetic inertia and fast frequency response approaches are tested and discussed.

Index Terms—Ancillary services, controllable loads, fast frequency response, frequency support, microgrid, power hardware-in-the-loop, street lighting, synthetic inertia.

I. INTRODUCTION

DUE to the replacement of conventional generation with Renewable Energy Sources (RES), in future years, Ancillary Services (AS) for power system management will also have to be provided by Distributed Energy Resources (DERs) and controllable loads located at the distribution level [1]. With this aim, several papers and research projects investigated how such resources could be employed as *flexibility resources* to provide AS like frequency and voltage regulation [2], as well as to solve congestion issues [3], [4].

Manuscript received 25 May 2022; revised 5 October 2022; accepted 8 November 2022. Date of publication 23 November 2022; date of current version 20 March 2023. Paper 2022-PSEC-0234.R1, presented at the 2021 IEEE International Conference on Environment and Electrical Engineering and 2021 IEEE Industrial and Commercial Power Systems Europe, Bari, Italy, Nov. 03, and approved for publication in the IEEE TRANSACTIONS ON INDUSTRY APPLICATIONS by the Power Systems Engineering Committee of the IEEE Industry Applications Society. The work of Dr. Bruno was supported by Regione Puglia through the framework of the Programme REFIN - Research for Innovation under Grant #A1C03120. (*Corresponding author: Cosimo Iurlaro.*)

The authors are with the Department of Electrical and Information Engineering (DEI), Politecnico di Bari, 70125 Bari, Italy (e-mail: sergio.bruno@poliba.it; giovanni.giannoccaro@poliba.it; cosimo.iurlaro@poliba.it; massimo.lascala@poliba.it; marco.menga@poliba.it; carmine.rodio@poliba.it; roberto.sbrizzai@poliba.it).

Color versions of one or more figures in this article are available at <https://doi.org/10.1109/TIA.2022.3223964>.

Digital Object Identifier 10.1109/TIA.2022.3223964

However, since DERs based on power electronic converters are electrically decoupled from the power grid and, then, are not provided with physical inertia or damping properties [5], they cannot contribute to transient stability. The parameter of inertia represents the amount of kinetic energy that rotating machines are able to store and release to the system in correspondence of sudden power imbalances [6]. With an increasing amount of non-synchronous generation, the whole system inertia decreases, leading to larger frequency excursions and system instabilities [7]. Assuming the frequency gradient as a measure of the power system weakness, with respect to withstanding sudden power imbalances [6], this risk of collapse is also more evident for small-sized power systems, like islands and smaller synchronous areas [8], [9]. In such cases, system operators have less time to react due a higher RoCoF [10]. Therefore, limiting transient frequency deviations results crucial to avoid situations that can be dangerous for system stability, like generators trip, unwanted load shedding intervention, etc. [6].

Several authors investigated how AS like Synthetic Inertia (SI) and Fast Frequency Response (FFR) options can be effectively employed as grid services to limit RoCoF and control supply-demand imbalances [5], [11]. A few papers investigated the possibility to provide SI or FFR by means of domestic thermal loads as refrigerators/boilers [12], [13] and variable speed heat pumps [14]. Other studies focused on providing such grid services through the advanced control of single phase electric vehicles [15] and Battery Energy Storage System (BESS) [16], [17], [18]. In [19], the fast primary frequency regulation of a dual-BESS scheme was investigated considering also the coordination with the ramping behaviour of conventional generators.

Hybrid solutions of FFR and SI actions have been also proposed, as in [20], in which an optimal control strategy of a hybrid battery/supercapacitor storage system was presented. Among other various solutions proposed in the literature, as specified in [21], [22], dimmable lighting systems represent competitive resources to be employed to provide AS in a Demand Response (DR) framework. Light-Emitting Diode (LED) lamp technologies are very promising from this point of view since they can be rapidly regulated by using remote or local control signals. Several studies and projects demonstrated how controlling networked LED streetlights is possible in the monitoring and control framework of smart grids [23], to provide demand side managements services or optimize energy use through the integration with other urban energy infrastructures such as EV

charging stations ([24], [25]). In addition, dimmable lighting systems can be used for DR as long as illuminance variations are adequately controlled and, then, still acceptable by final users [26]. In [27], the authors demonstrated how SI can be provided by LED lamps without having to add significant BESS or supercapacitors, but simply connecting a DC link capacitor to the LED lamps. The use of LED lighting system to support BESS [28] and conventional generators [29] during primary frequency regulation has also been shown. Examples of LED control strategy aimed to provide primary/secondary frequency regulation have also been described in [30], [31]. Nevertheless, these last solutions are based on a decentralized control strategy, with the drawback to require a relevant number of controllers to be installed, one for each lamp, to gather a significant amount of flexibility.

In [32], the authors made a preliminary and successful assessment of the feasibility of providing SI and FFR support through the centralized control of public LED street lighting systems. Test results were obtained considering the response of an actual LED lamp in a Power Hardware-in-the-Loop (PHIL) test bed. However, these tests were carried out considering a simplified single-bus electromechanical model of the power system, neglecting the representation of main grid components, such as lines or transformers. As shown in [33], the presence of grid impedances among regulating resources can affect the overall transient response. Therefore, in this paper, the study in [32] is extended and completed as follows:

- additional PHIL tests have been carried out adopting a more accurate system model, which reproduces the behavior of main electrical devices and components of an actual non-synchronous power grid;
- the adopted power system model is detailed enough to describe the influence of high impedance LV circuits, MV/LV transformers and the actual voltage and power controllers used in a power plant;
- the response of multiple LED lighting systems connected in different locations was considered in order to build a more accurate system scenario and keep into account the electrical distance of the distributed sources;
- further tests have been performed to assess the impact of the proposed LED lighting system control scheme in various scenarios of growing severity;
- a more detailed description of the SI and FFR controllers and of the Power Hardware-in-the-Loop set-up have been added.

The grid modelled for these studies represents the MV/LV distribution system of an actual small Italian island, not connected to the main grid. There are multiple rationales under this choice. In the next few years, Italian small islands will continue to be challenged in embracing a significant transformation of their energy generation and network assets [34]. With the mandatory installation of a minimum amount of intermittent renewable sources, small non-synchronous islands, which are inherently characterized by low rotational inertia, will suffer further reductions of inertia and experience harsher frequency events. Therefore, it is essential to develop new ways of ensuring frequency quality, even resorting to demand response approaches.

In addition, the adoption of a small-sized test system also allows to ensure suitable details, while respecting the strict computation time requirements of real-time simulations and PHIL tests.

II. FLEXIBLE CONTROL RESOURCES THROUGH LED STREET LAMPS

With LED technologies getting less and less expensive by the day, LED lamps are progressively substituting all others in both new installations and refurbishment projects. Their competitive performances in terms of efficiency, life expectancy, reliability, controllability and Electromagnetic Compatibility (EMC) impacts make them one of the lead technologies in public street lighting systems. According to the standard [35], if a “Full Adaptive Installation” is employed, the *lighting class* of street lamps can be reduced during low traffic conditions. *Lighting classes*, as defined by the Part 2 of the European standard EN 13201:2015 [36], determine the road lighting conditions to be ensured to guarantee the safety of road users. Illuminance control actions are allowed, as long as they comply with minimum standard requirements.

Various techniques can be used to easily control and dim LED lamps. For example, the *0-10 V_{DC} protocol* is widely adopted for analog dimming. According to this protocol, the lamp scales its light output so that at a control voltage of 10 V its light intensity corresponds to 100% of its rated value, while below 1 V its light intensity is at its minimum value. However, this control technique is not prone to be extended to control several lamps distributed in a large geographical area.

Several protocols, already commercially available, permit to control a larger number of LED drivers. For example, *DALI* controllers allow to manage up to 64 LED lamps, at a maximum distance of about 300 meters. However, time specification of this kind of controllers might not be adequate for applications requiring a very fast device response. The *DMX-512* technology allows instead to control up to 512 networked devices, at a maximum distance of about 300-500 meters, theoretically extendable using repeaters. Since the transmission time for a maximum sized packet with 512 channels is about 20 ms, this protocol is fast enough to be employed for fast modulation of the light output of LED lamps. Clearly, the use of *DMX-512* implies the installation of a wired communication system among all lamps.

The applicability of wireless controllers has been also proved in [23], where each LED lamp in a networked lighting system has been provided due to a receiver that can collect data packages sent via radio transmission at a frequency of about 900 MHz. GPS applications for the control of lighting systems are also patented. Large geographical areas are therefore theoretically reachable by the same control system, although the easiest solution could be implementing local frequency measure and control at each lighting control box that usually manages few dozens of street lamps. An example of low-cost synthetic inertia local controller has been studied by the authors in [16].

The implementation of these solutions could be prohibitive in practical applications if the infrastructure is implemented only for frequency support, due to the high investment costs associated with the communication infrastructure, especially if

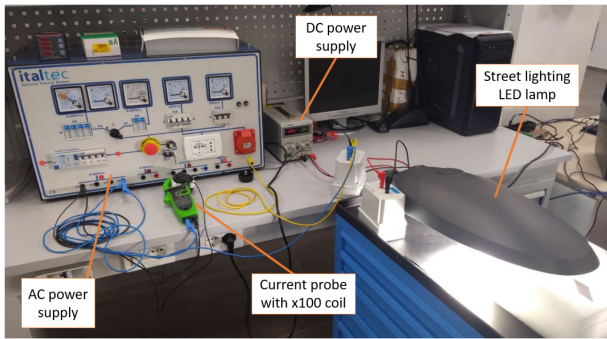


Fig. 1. Set-up for the LED street lamp characterization tests.

implemented over large geographical areas. However, it could be applied to pre-existing infrastructures (without significant additional costs) and to smart grids in which the remote control of DERs if already implemented (e.g. for energy optimal control) and could be extended to SI and FFR.

In this paper, the real-time control of LED street lamps is proposed to harvest flexible resources for fast frequency regulation. Since the most severe part of a frequency transient is usually extinguished within few seconds from its onset, the time activation of LED lamps control is a crucial aspect in the feasibility of the proposed control. The need of a very fast response introduces for sure some drawbacks in the proposed control scheme, although it also brings some advantages. Given the very short duration of frequency transients, the visual impacts due to this kind of control can be considered comparable to the fluctuations that can be observed during commonly experienced disturbances of power quality such as deep voltage sags or transient voltage interruptions. Due to the very strict requirements in time response, the proposed LED lamp control will be tested in a real-time environment through a Power Hardware-in-the-Loop test bed. The paper presents the experimental results obtained by regulating the power output of an actual LED street lamp according to different frequency-dependant control laws.

A. Characterization of the LED Lamp Power Regulation Response

The first tests were aimed at drawing the control characteristic curve of the LED street lamp. The lamp used for these tests is a commercially available product, which is controlled by a LED driver through a direct current (DC) regulating signal in the range 0–10 V. The higher the DC voltage, the higher luminous flux is produced by the lamp, and the higher is the electric power absorbed. The control characteristic was obtained through the experimental results collected from the test setup shown in Fig. 1. The LED lamp was fed by an AC power source supply, whereas a DC power supply was used to regulate the DC voltage input to the LED driver. The absorbed current was measured using a current probe coupled with a $\times 100$ coil to amplify the current signal.

The results obtained by controlling the LED driver with a voltage ranging in the interval 0–10 V have been collected in Table I. These same results are also shown graphically in Fig. 2

TABLE I
TEST RESULTS

Voltage [V]	Current [A]	Power [W]
0.0	0.06	13.1
0.5	0.06	13.1
1.0	0.06	13.1
1.5	0.07	16.2
2.0	0.10	22.7
2.5	0.13	29.3
3.0	0.16	36.0
3.5	0.19	42.4
4.0	0.22	49.4
4.5	0.25	56.0
5.0	0.28	62.8
5.5	0.31	69.7
6.0	0.34	76.7
6.5	0.37	83.6
7.0	0.40	90.6
7.5	0.43	97.4
8.0	0.46	103.6
8.5	0.46	103.6
9.0	0.46	103.6
9.5	0.46	103.6
10.0	0.46	103.6

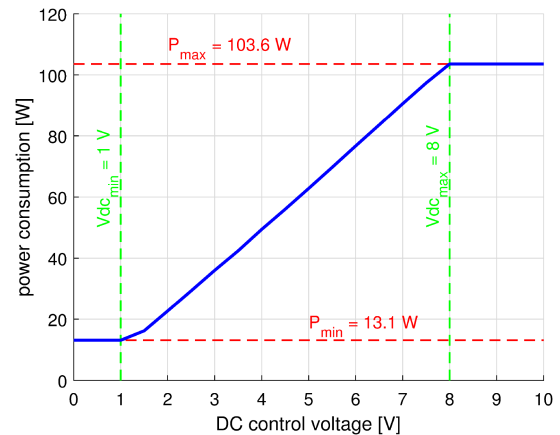


Fig. 2. Power-Voltage characteristic curve of the LED Street Lamp.

where the LED lamp power consumption is represented as a function of the DC voltage control input. It can be observed that voltage inputs below 1 V and above 8 V do not produce any significant variation in terms of both absorbed power and luminous flux. Therefore, 1–8 V is the regulating interval that will be used to control the lamp during future tests. In this interval the characteristic curve appears to have almost a linear behavior. In these tests, the lamp was supplied with the nominal voltage 230 V. However, other tests, not shown here for the sake of brevity and carried out by changing the voltage magnitude of the power supply, showed that the lamp power consumption is scarcely influenced by the voltage within a large confidence interval (200–250 V).

According to the experimental results, the lamp under test can be regulated to absorb an electric power ranging from a maximum of 103.6 W to a minimum of 13.1 W. This means that the lamp can be dimmed in order to reduce its consumption by about 90%, when the lamp is operating at full power. Lamps which operate at half capacity, for example in certain

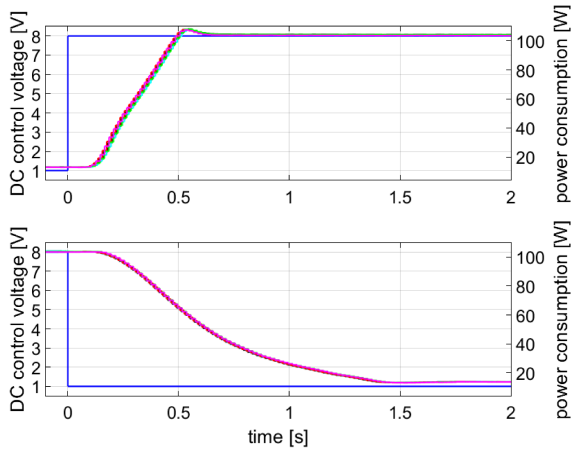


Fig. 3. Response of Upward and Downward Load Regulation.

periods of the night when the reduced traffic conditions permit to downgrade the lighting class, could instead theoretically provide instantaneous power control for both upward and downward regulation.

Further tests were carried out in order to characterize the LED lamp time response to a DC control voltage step change, and verify if this control is fast enough to be applied for fast frequency regulation. Fig. 3 shows the results obtained by controlling the lamp from one of the extremes of the characteristics curve (Fig. 2) to the other, during both upward and downward regulation. In both subplots, the blue curve represents the step-change variation given to the DC control voltage. Each graph contains also multiple active power responses, which almost overlap, obtained repeating the same test multiple times.

The component is clearly characterized by an asymmetrical response, with a faster step-change response observed during upward load regulation. Further tests, not shown here for the sake of brevity, conducted by selecting different step change sizes and initial operating point, showed a more or less constant delay in the 400–500 ms range during upward load regulation, and a delay ranging in the interval 500–1400 ms for downward regulation. The maximum delay was observed when the lamp has to go from maximum to minimum power. This is clearly a critical issue in FFR applications, since the delay inevitably reduces the effectiveness of the proposed control. However, this behaviour permits to limit the sudden change in illuminance, minimizing the visual disturbances to humans and possible hazards to road safety.

III. POWER GRID MODEL OF A SMALL NON-INTERCONNECTED ISLAND

The possibility of providing fast frequency support through LED street lamps was preliminary investigated in [32], demonstrating how improvements in terms of frequency behaviour can be obtained. Tests were performed adopting a very simplified electromechanical single-bus model, whereas, in this paper, a more accurate evaluation is given through the development of a detailed power system model for real-time simulations and

TABLE II
MAIN CHARACTERISTICS OF THE GRID COMPONENTS

S_n [kVA]	TR1	TR2	TR3	TR4	TR5
V_{1n} [kV]	2000	400	630	250	630
V_{2n} [kV]	10.0	10.0	10.0	10.0	10.0
$P_{cc}\%$	0.4	0.4	0.4	0.4	0.4
$P_{cc}\%$	0.91	1.15	1.04	1.15	1.04
$P_{fe}\%$	6.0	4.0	4.0	4.0	4.0
$P_{fe}\%$	0.14	0.21	0.18	0.25	0.18
$I_0\%$	0.9	1.3	1.1	1.3	1.1
P_n [kW]	RL1	RL2	RL3	RL4	RL5
V_n [kV]	1810	590	700	300	650
	0.4	0.4	0.4	0.4	0.4
$Length$ [km]	MVL1	MVL2	MVL3	MVL4	MVL5
r_l [Ω/km]	0.510	0.510	0.510	0.850	0.510
x_l [Ω/km]	0.387	0.387	0.387	0.253	0.387
	0.086	0.086	0.086	0.120	0.086

PHIL tests. The model proposed for this test is based on the actual MV and LV distribution network that supplies energy in an Italian small island.

The modelled distribution grid is structured as in Fig. 4. It mainly consists of five 10 kV MV buses, each one connected through a transformer to a LV bus. Five distribution lines connect the MV nodes, creating a loop that is normally open during operation. Each LV bus supplies electricity to (mostly) residential customers, which have been represented through the equivalent loads RL1-RL5. The installed load capacity P_n at each node is reported in Table II. One of the LV node (bus #1 in Fig. 4) supplies the largest number of customers (RL1) and is connected to a generation plant with a 2000 kVA rated power and 50 Hz frequency. The plant is based on a set of diesel generating units and supplies electricity to the local load and to the rest of the island via an elevator transformer (TR1). It should be noted that the detailed model of the generating unit has been represented considering all voltage and mechanical power regulators, a detailed model of the synchronous machine and prime mover dynamics.

Since the proposed control is based on the real-time management of the public LED street lighting system, each LV node was also connected to an additional equivalent circuit, which represents a portion of the street lighting system used to light the entire island. More details are given in the subsection below.

The real-time model of the distribution grid is based on a detailed three-phase representation. All system components were modelled using the libraries available in the real-time simulator programming environment. Each component was modelled according to the parameters listed in Table II. These values have been obtained from the data sheets of the components actually installed on the island. Residential loads (RL1-RL5) do not normally participate to frequency control and, therefore, were modelled using a constant PQ model. This choice permits to simplify the model and reduce the computational efforts required during real-time simulations. A dynamic load model was used instead to represent the power consumption at the street lighting system nodes. Loading levels were set to reproduce conditions of low consumption, usually experienced during the night and far from the tourist season, when the island is more populated. Due to the scarce loading level, the number of active generators is low

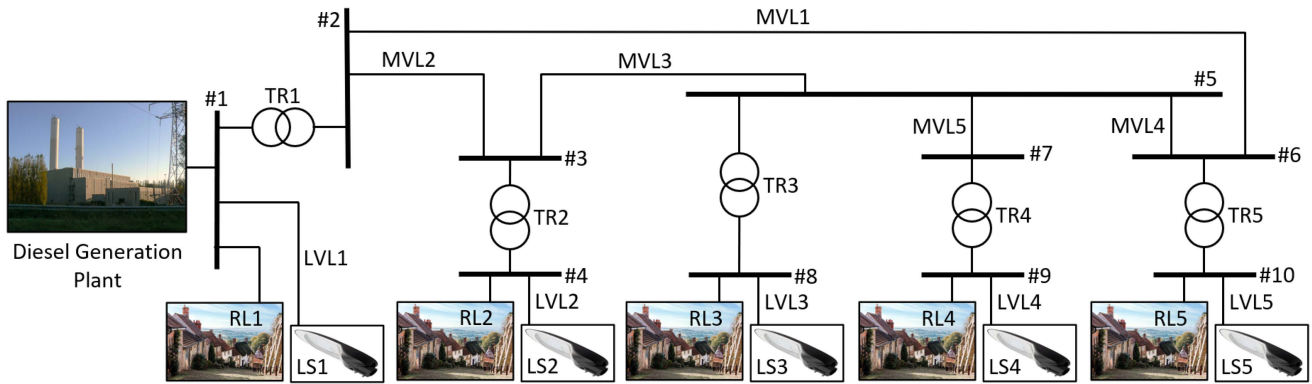


Fig. 4. Modelled small islanded distribution grid.

TABLE III
POWER AND NUMBER OF LAMPS AT EACH LV NODE

	LS1	LS2	LS3	LS4	LS5
P_{LS} [kW]	24.20	7.76	9.32	4.04	8.69
$N.$ of lamps	234	75	90	39	84

and the rotational inertia is much reduced. Low inertia conditions can also be due to high RES production and consequent decrease of the number of active synchronous machines.

A. Model of the LED Street Lighting System

The street lighting system has been modelled according to some assumptions. The installed power of the simulated street lighting system was estimated using aggregated data at national level. According to the statistics in [37], in 2017, the electricity consumption of public lighting in Italy was about 6000 GWh. Assuming that the public lighting lamps are usually switched on less than half a day (about 4000 hours per year) and that they work almost all times at their rated power, it appeared reasonable to consider that the installed power of the lighting systems in Italy in that year was about 1.5 GW. This value is about 3% of the national load peak (55 GW in 2017, as reported in [38] by the Italian TSO). Applying the same percentage to the simulated system, whose peak power demand is about 1.8 MW, it is possible to assume that the installed power of the public street lighting system in the island is about 54 kW.

Having estimated the overall load for street lighting and the total number of lamps, it was assumed to distribute such load on five subsystems, connected at the LV system nodes. The number of lamps for each subsystem is proportional to the installed load capacity at LV level. As represented in Fig. 4, each lighting subsystem is modelled using an equivalent three-phase load (LS1-LS5), supplied by an equivalent low-voltage distribution line (LVL1-LVL5). Table III shows equivalent power and number of installed lamps for each street lighting subsystem (LS1-LS5).

The equivalent lines LVL1-LVL5 were modelled assuming typical lengths in urban applications and according to the actual data of the urban lighting system in [25]. Cross-section of cables

TABLE IV
CHARACTERISTICS OF THE EQUIVALENT DISTRIBUTION LINE OF THE LIGHTING SUBSYSTEMS

	LVL1	LVL2	LVL3	LVL4	LVL5
$Length$ [km]	0.81	0.78	0.93	0.42	0.87
$N.$ of circuits	3	1	1	1	1
$Cross-sections$ [mm ²]	4x25	4x25	4x35	4x6	4x25
r_l [Ω /km]	0.99	0.99	0.71	4.21	0.99
x_l [Ω /km]	0.093	0.093	0.089	0.114	0.093

were sized to avoid excessive voltage drops at the terminal of each lighting circuit. The adopted values are summarized in Table IV. Please, consider that due to the large number of lamps assigned to LS1, this street lighting system was divided into three parallel sub-circuits, each one supplying one third of the total LS1.

IV. SYNTHETIC INERTIA AND FAST FREQUENCY RESPONSE MODELS

In order to investigate the support that LED street lamps can provide to enhance the grid frequency behavior, two frequency-dependant control laws have been proposed, namely *Synthetic Inertia* or *Fast Frequency Response*. These two approaches have never been applied or tested on LED urban lighting systems. An approach somewhat close to what we have proposed was found in [27]. The authors in [27] evaluated the possibility to provide virtual inertia through the energy stored in the capacity of the DC-link that supplies the LED lamp. Due to the limited capability of the DC-link of the lamp driver, this technique can provide a very limited power respect to the SI control proposed in our work that can control up to 90% of the LED lamps rated power (see Subsection II-A). On the other hand, for FFR control, a possible comparison can be done in relation to other primary frequency controls with LED lamps proposed in the literature. The FFR control law in our work is comparable to the controls in [28] and [31]. In these works, however, the actual response and characteristics of LED lamps and their drivers were not considered. In our work, instead, thanks to the PHIL implementation, the behaviour of an actual (commercially available) LED street lamp, with its driver and control system, was thoroughly taken into account. A different control law is proposed in [30]

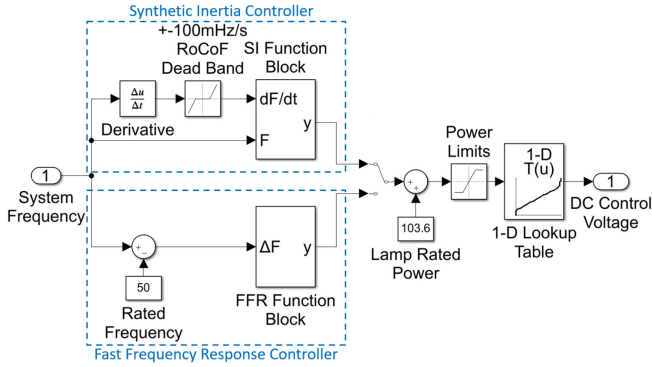


Fig. 5. Synthetic inertia and fast frequency response control scheme.

to provide primary frequency support by LED lighting systems. However, this control introduces a fixed delay to reduce the frequency control activation in addition to a dead-band on the frequency deviation. The introduction of this delay does not permit to obtain a prompt response of the devices for very severe contingencies.

A scheme of the SI/FFR controller used for tests is given in Fig. 5 where, through a control switch, it is possible to choose the control law to be adopted. The output of the controller is the amount of load to be curtailed. The curtailed load set-point is converted into a DC control voltage set-point using the look-up table obtained during the characterization tests in Section II (see Fig. 2). The DC control voltage obtained in this way is applied to the LED driver to regulate the luminous flux, and therefore the power supplied to the lamps. A detail of the SI and FFR function blocks in Fig. 5 is given in the next subsections. Please note that, for the sake of simplicity, in this paper, it was assumed to allow SI/FFR control of the street lamps only during underfrequency events, when lamps are working at their maximum power and their power output can only be regulated downward. However, it is possible to imagine that a symmetrical control of loading power could be implemented on the lamps that are working at half capacity during reduced road traffic conditions.

A. Synthetic Inertia Control Law

As reported in [39], synthetic inertia is obtained by applying a control law proportional to the frequency derivative (RoCoF). Some applications of this control are reported in [40], [41]. However, a control law that follows continuously the RoCoF trajectory can lead to a rise in the frequency response settling time, because of the inertial support given after having reached the *nadir* point. Such drawback can be overcome by adopting the solution proposed in [42] where the SI control is applied only when RoCoF and frequency deviations have the same sign. The SI control adopted in this paper is similar to the one proposed in [42], although, in this case, having modelled also secondary frequency regulation, the steady-state value is given by the nominal frequency (50 Hz). As shown in Fig. 5, a RoCoF dead band of ± 100 mHz/s has also been introduced in order to avoid unnecessary regulations, due for example to measurement noise. Indeed, RoCoF calculation can be affected by large errors

due to noise on frequency measurement. To further reduce the effect of noise, a low-pass filter can be applied to the frequency measurement. According to the step-change responses shown in Fig. 3, the dynamic behaviour of the controlled LED lamp is characterised by a large delay and is therefore inherently less susceptible to noise, making the use of a filter unnecessary. Assuming F as the frequency sample at the time t and K_{SI} as the applied gain factor, the SI control law implemented in the *SI Function Block* consists of the following *if statement*:

$$\begin{cases} \text{if } F \leq 50 \ \& \ dF/dt < 0.1 \\ \quad y = K_{SI} \cdot dF/dt \\ \text{else} \\ \quad y = 0 \end{cases}$$

According to this rule, a non-zero output y of the SI controller is obtained only when the frequency is below its nominal value (50 Hz). The gain factor K_{SI} was sized so that the maximum power variation is obtained when a 0.5 Hz/s RoCoF is reached.

B. Fast Frequency Response Control Law

As defined in [39], the fast frequency response aims to provide grid support for reduced inertia systems by means of units able to quickly respond to frequency excursions, with an active power response proportional to the frequency deviation. Assuming ΔF as the measured frequency deviation from the steady-state value, and introducing a 0.1 Hz dead-band to avoid excessive stress to the lamp, the control output y of the *FFR Function Block* in Fig. 5 is formulated as follows:

$$\begin{cases} \text{if } \Delta F \leq -0.1 \\ \quad y = K_{FFR} \cdot (\Delta F + 0.1) \\ \text{else} \\ \quad y = 0 \end{cases}$$

The gain factor K_{FFR} has been set in order to obtain the maximum power contribution with frequency deviations greater than 0.5 Hz.

V. TEST RESULTS

This section describes the set-up for the Power Hardware-in-the-Loop experimental tests and discusses the results obtained considering the SI and FFR control strategies.

A. Power Hardware-in-The-Loop Test Bed Architecture

The PHIL set-up used to investigate the effectiveness of the proposed SI and FFR controls is shown in Fig. 6. It consists of a real-time digital simulator (OPAL RT5600), a power amplifier module, managed by an amplifier controller, and a real LED street lamp, whose physical response is applied in PHIL to the simulated power system. The real-time simulator, which was interfaced with the amplifier controller by means of an optical fiber channel, simulated both the distribution network described in Section IV and the LED lamp controller. The DC-control voltage signal (0–10 V) sent to the LED driver to control the lamp luminous flux, was generated by the real-time simulator as an analog output, using the *hardware synchronized mode*.

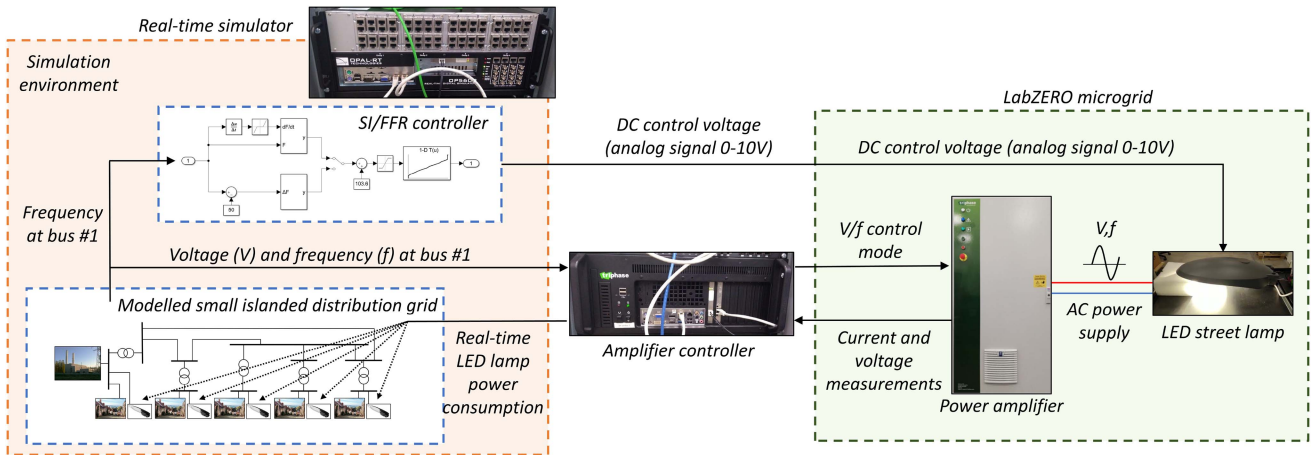


Fig. 6. Set-up of the Power Hardware-in-the-Loop simulation tests.

The LED lamp was connected to the LabZERO microgrid at the Politecnico di Bari, which was supplied by the programmable power source operating in voltage source control mode. According to this set-up, frequency and voltage signals of the simulated non-synchronous system were communicated to the amplifier controller and, then, physically applied to the microgrid busbar. The response of the microgrid (and the LED lamp) to the frequency and voltage variations is measured by the programmable power source and transformed into a PQ signal to be fed back to the real-time simulation.

These active and reactive power signals were suitably scaled to reproduce the response of the five street lighting subsystems connected at different LV nodes. Thanks to the characterizations tests, it was proved how LED lamps behavior was not influenced by voltage magnitude in a very large interval. Therefore, the expected response of all simulated lamps can be considered similar to the physical LED lamp as long as the frequency is the same on the entire grid. This condition can be considered true since the system is very small in size and is supplied only by a single power plant.

B. Case 1. SI Control of LED Lamps

The proposed SI control was tested applying a sudden load step variation of 180 kW to the simulated grid, in a day characterized by an average power consumption of about 1.25 MW. Given the very low rotational inertia of the diesel power plant (assumed to be 0.3 s with respect to the maximum installed power 2000 kVA), the frequency transient following this disturbance, applied at the generic time $t = 0$ s as in Fig. 7, shows a very steep descent with an initial RoCoF higher than 8 Hz/s, and a nadir of about 48.3 Hz, much lower than the 49 Hz minimum suggested by the standard EN-50160 for the quality of frequency in systems with no synchronous connection.

Fig. 8 shows how the proposed SI controller can generate a DC control signal adjusting the active power consumption of the LED lamps during the frequency transient. The effect of this control action is visible in Fig. 7 with a non negligible contribution to the nadir, which is now raised to about 48.4 Hz,

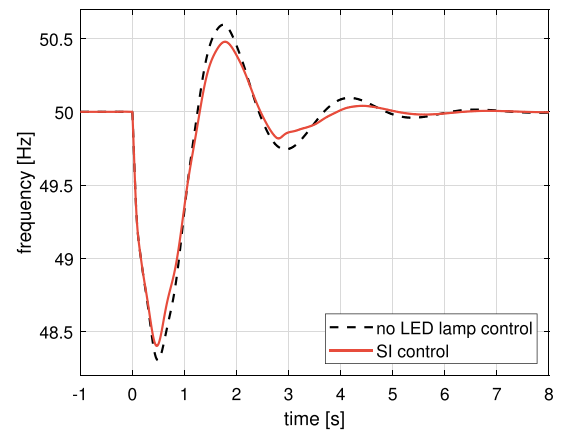


Fig. 7. Case 1. Frequency response with SI control.

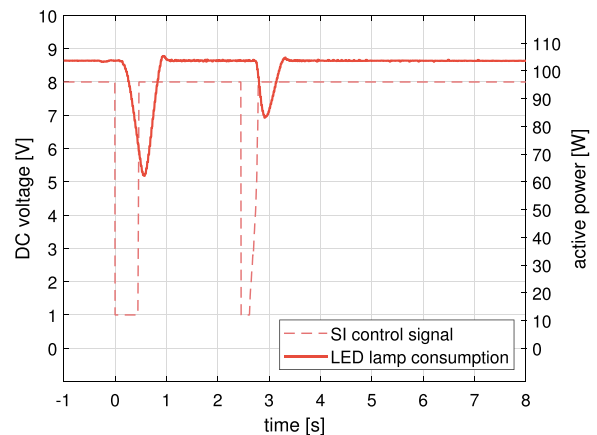


Fig. 8. Case 1. LED lamp response with SI control.

a reduction of the frequency overshoot and an overall quicker settling time.

As shown in Fig. 8, due to the high RoCoF, a maximum power reduction was instantly asked to the LED lamps. Within few hundred of milliseconds the LED lamps began to reduce

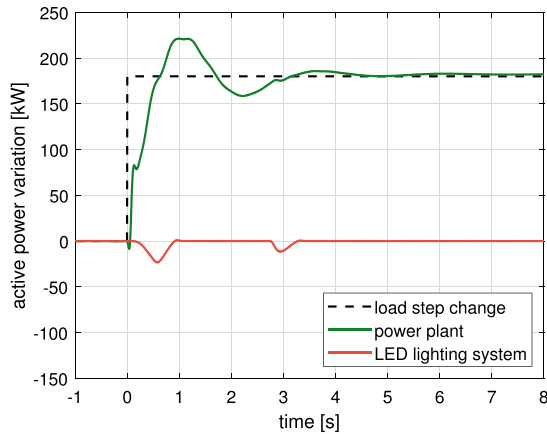


Fig. 9. Case 1. Active power response with SI control.

their consumption. The SI controlling signal was stopped after having reached the nadir, and the lamps went back to their regular operating point within a second from the start of the disturbance. Due to the severity of the transient, a second activation of SI was also requested during a second oscillation.

Fig. 9 shows how the power response provided by the diesel generation plant derives from a detailed model of the generating units. Its response is clearly much more significant than the LED lamps, whose consumption is in this case only just about 4% of the overall load. Furthermore, due to the high speed of the system response, the contribution of the lamps to the dynamics can be exploited for a short time only. However, it should be observed that these tests were carried out on particularly stressed conditions. In fact, the model of the non-synchronous system was characterized by an extremely low amount of inertia. The frequency support could have been more significant in system with more inertia and, then, a delayed nadir time. Nevertheless, from another point of view, the limitation in the active power control of the LED lamps guarantees that the visual impact during the transient is very limited.

C. Case 2. FFR Control of LED Lamps

This second case is equivalent to the previous one, but this time the presence of a FFR control of the LED lamps was assumed. Fig. 10 shows the system frequency response with and without the FFR support. The response is quite similar to the previous case, although a better control of the frequency overshoot and settling time is obtained. Fig. 11 shows the LED lamp power response and the control signal applied to its driver.

By comparing the two trends in Fig. 8 and Fig. 11, it is possible to observe that the FFR control strategy is slightly delayed, but allows a longer activation of the LED lamp active power control. This is due to the fact that, in general, when an imbalance occurs, the RoCoF (dF/dt) reaches instantaneously its maximum value, saturating the SI control, and goes rapidly to zero when the nadir is reached. Frequency deviation (ΔF), instead, starts from zero and needs more time to reach the saturation threshold of FFR control (set in this case at -0.5 Hz). FFR control is requested until ΔF is brought back within the dead-band limits (i.e. at 49.9 Hz), with an overall activation of about 1 s. In this case,

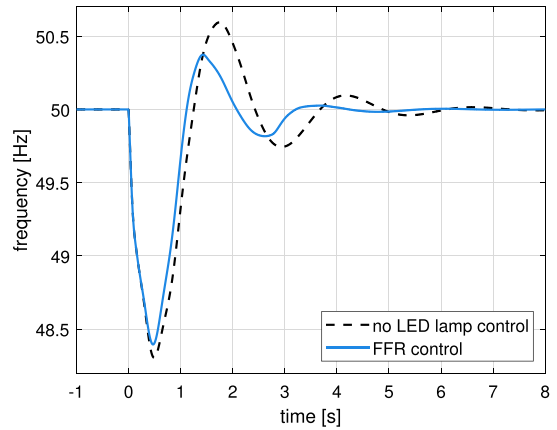


Fig. 10. Case 2. Frequency response with FFR control.

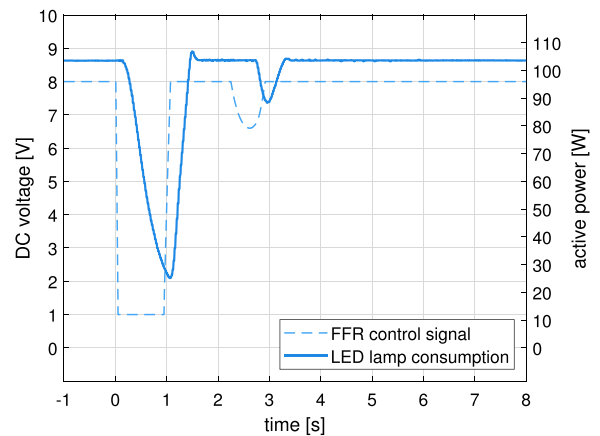


Fig. 11. Case 2. LED lamp response with FFR control.

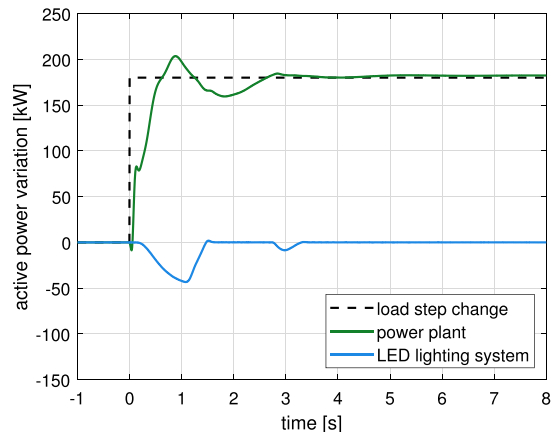


Fig. 12. Case 2. Active power response with FFR control.

the LED lamps have enough time to curtail almost all of their consumption, ensuring higher damping and a smaller frequency overshoot. Nadir point is comparable to the one reached with SI inertia control, although just slightly lower. Fig. 12 shows the active power response of both diesel generation plant and LED street lighting systems.

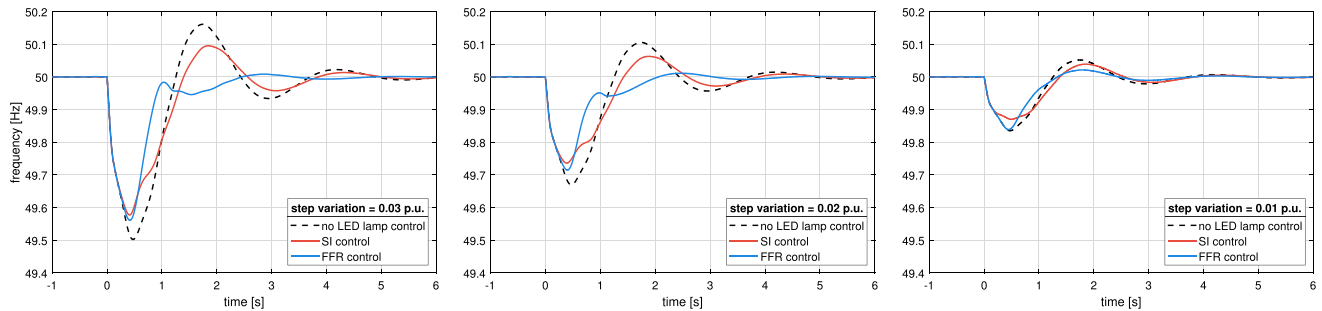


Fig. 13. Cases 3-5. Frequency response to a 3% (left), 2% (center) and 1% (right) load variation.

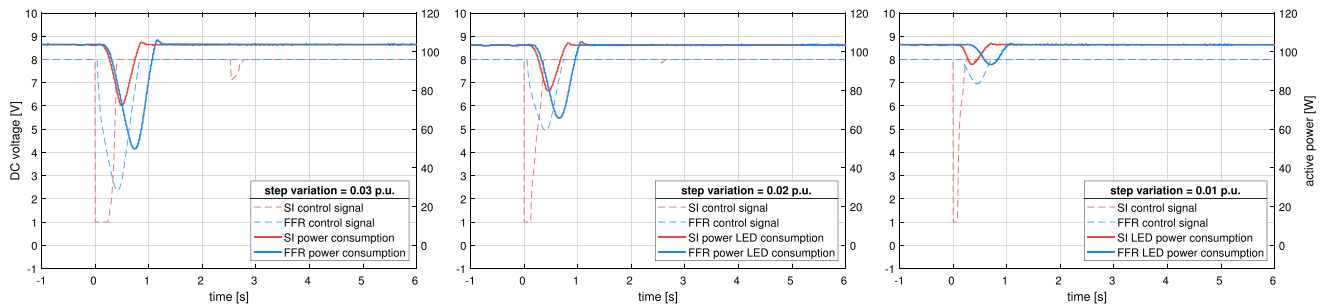


Fig. 14. Cases 3-5. LED lamp response to a 3% (left), 2% (center) and 1% (right) load variation.

D. Cases 3-5. Further Comparison of SI and FFR Control

The previous tests assumed a very severe contingency, with values of RoCoF and frequency deviations which rapidly saturated either SI or FFR control. Further tests have been carried out in order to investigate the response of SI and FFR control laws in absence of saturation.

Fig. 13 allows to compare the system frequency response obtained with SI and FFR control, applying gradually smaller load step variations. The three cases, namely 3, 4 and 5, are characterized by a 3%, 2% and 1% load variation, respectively. In these cases, the SI controller allowed to improve more visibly the response in terms of nadir with respect to the FFR. With the decreasing of the disturbance severity, RoCoF decreases and the FFR control is activated with larger delays, because of the time necessary for the frequency deviation to reach the dead-band lower limit. In all cases, however, FFR control allows to limit or even avoid the frequency overshoot.

In addition, having imposed a load variation in the system equal to the installed power of the public street lighting system in the island (3% of the total load), the proposed controls allow to reduce the maximum frequency deviation by 20%. This reduction, using the SI control, increases if the load step change has a magnitude lower than the controlled LED-lamp power volume. Indeed, SI control, being based on RoCoF, is able to provide a contribution even for very modest contingencies. For this reason, SI controller can be considered preferable as it can provide a better counter-balance for the smaller load variations that most often occur during normal grid operation.

Fig. 14 shows the DC control voltage set-points generated by SI and FFR in the three cases, together with the LED lamps active power response. It is possible to observe that, due to the extremely low system inertia and the high values of initial

RoCoF, even during small disturbances, SI control is still characterized by a sort of on/off behavior. The FFR control signal, instead, changes more smoothly. However, due to the actual delays in the response of the LED lamp, observed during the characterization tests presented in Section II, the active power response follows initially about the same trajectory, with just a little delay in the case of FFR. The main difference of the two controls is again found in the longer activation time of the FFR control. As also previously remarked the delayed response of the lamp allows in any case to minimize the visual impacts which can be considered negligible.

VI. CONCLUSION

The article explored the idea of using LED public street lighting systems to obtain an extra grid support in scenarios characterized by very low rotational inertia. The capability of providing a very fast active power regulation, without disconnecting the lamps, was investigated through Power Hardware-in-the-Loop tests. PHIL tests allowed to integrate the simulation of a MV/LV isolated distribution grid with the behaviour of an actual LED street lamp controlled to provide both SI or FFR control actions.

The simulated grid represents the non-synchronous power system of an actual small Italian island, comprising all main MV/LV components, a detailed diesel generation power plant and a distributed public street lighting system. This kind of non-synchronous systems is inherently characterized by low total inertia, and will face in the next years the challenge of integrating larger and larger amount of RES, with further expected reduction of inertia.

The proposed LED lamp control was tested in a scenario characterized by an extreme reduction of inertia, allowing to

prove how a non-negligible contribution to frequency support can be obtained exploiting these controllable resources. Clearly, having limited power with respect to the overall load and being characterized by delays assessed between 400 and 1400 ms, LED lamps cannot substitute other active components, such as batteries or fly-wheels. However, the tests showed how, if suitably controlled, LED lamps can be considered as additional widespread resources to be exploited for supporting the grid and reduce the capacity of other controlling devices.

The PHIL tests showed that FFR control, in case of severe contingencies, allows a more pronounced contribution to enhance the frequency behavior but causes a longer drop in the illumination flux, which has a higher visual impact. On the other hand, SI control has the advantage of reducing impacts on illumination levels, due to a shorter activation time of the dimming control. For this reason, the SI control is preferable with regard to the use of LED street lighting systems to provide AS. In both cases, however, the visual impacts due to the control can be considered negligible and comparable to the same disturbances that can be observed during commonly power quality events, such as deep voltage sags or transient voltage interruptions, which happen hundreds of times in a year (more often than frequency events).

Entity and number of control actions can be reduced by downsizing the gains of the two controllers and increasing the dead bands, respectively. In the paper, the gains were chosen in order to produce an effective control action for most of the test cases presented. No particular problems in terms of stability or interaction with the other controllers were observed, mostly because of the limited power that can be controlled by the lighting systems, even in the case of saturated control laws. However, in practical implementations, the gains can be set according to the typical inertia and droop values adopted in power systems or specified by the national grid codes for the connection of active end-users.

REFERENCES

- [1] G. Migliavacca, "Introduction," in *Proc. TSO-DSO Interact. Ancillary Serv. Electricity Transmiss. Distribution Netw.: Model., Anal. Case-Stud.*, G. Migliavacca, Ed., 2020, pp. 1–5.
- [2] Y. Huo and G. Grusso, "Ancillary service with grid connected PV: A real-time hardware-in-the-loop approach for evaluation of performances," *Electronics*, vol. 8, no. 7, 2019, Art. no. 809.
- [3] H. Gerard, E. I. Rivero Puente, and D. Six, "Coordination between transmission and distribution system operators in the electricity sector: A conceptual framework," *Utilities Policy*, vol. 50, pp. 40–48, 2018.
- [4] S. Bruno, G. Giannoccaro, C. Iurlaro, M. L. Scala, L. Notaristefano, and C. Rodio, "Mapping flexibility region through three-phase distribution optimal power flow at TSO-DSO point of interconnection," in *Proc. IEEE AEIT Int. Annu. Conf.*, 2021, pp. 1–6.
- [5] A. Delnooz, J. Vanschoenwinkel, E. Rivero, and C. Madina, "Deliverable 1.3-Definition of scenarios and products for the demonstration campaigns," Coordinet, Hamburg, Germany, Tech. Rep., Jul. 2019. [Online]. Available: https://private.coordinet-project.eu/files/documents/5d72415ced279Coordinet_Deliverable_1.3.pdf
- [6] ENTSO-E, "Frequency stability evaluation criteria for the synchronous zone of continental Europe," ENTSO-E, Brussels, Belgium, Tech. Rep., 2016. [Online]. Available: https://eepublicdownloads.entsoe.eu/clean-documents/SOC%20documents/RGCE_SPD_frequency_stability_criteria_v10.pdf
- [7] T. Kerdphol, F. S. Rahman, M. Watanabe, Y. Mitani, D. Turschner, and H. Beck, "Enhanced virtual inertia control based on derivative technique to emulate simultaneous inertia and damping properties for microgrid frequency regulation," *IEEE Access*, vol. 7, pp. 14422–14433, 2019.
- [8] ENTSO-E, "Need for synthetic inertia (SI) for frequency regulation," ENTSO-E, Brussels, Belgium, Tech. Rep., Mar. 2017. [Online]. Available: https://docstore.entsoe.eu/Documents/Network%20codes%20documents/NC%20RfG/IGD_Need_for_Synthetic_Inertia_final.pdf
- [9] F. M. Gatta et al., "Replacing diesel generators with hybrid renewable power plants: Giglio smart island project," *IEEE Trans. Ind. Appl.*, vol. 55, no. 2, pp. 1083–1092, Mar./Apr. 2019.
- [10] F. Milano, F. Dörfler, G. Hug, D. J. Hill, and G. Verbič, "Foundations and challenges of low-inertia systems (Invited Paper)," in *Proc. IEEE Power Syst. Comput. Conf.*, 2018, pp. 1–25.
- [11] P. Mancarella et al., "Power system security assessment of the future national electricity market," Melbourne Energy Inst., Melbourne, VIC, Australia, Tech. Rep., Jun. 2017. [Online]. Available: <https://www.energy.gov.au/sites/default/files/independent-review-future-nem-power-system-security-assessment.pdf>
- [12] F. Conte, M. Crosa di Vergagni, S. Massucco, F. Silvestro, E. Ciapponni, and D. Cirio, "Performance analysis of frequency regulation services provided by aggregates of domestic thermostatically controlled loads," *Int. J. Elect. Power Energy Syst.*, vol. 131, 2021, Art. no. 107050.
- [13] V. Trovato, I. M. Sanz, B. Chaudhuri, and G. Strbac, "Advanced control of thermostatic loads for rapid frequency response in great britain," *IEEE Trans. Power Syst.*, vol. 32, no. 3, pp. 2106–2117, May 2017.
- [14] I. Ibrahim, C. O'Loughlin, and T. O'Donnell, "Virtual inertia control of variable speed heat pumps for the provision of frequency support," *Energies*, vol. 13, no. 8, 2020, Art. no. 1863.
- [15] M. Rezkalla, A. Zecchino, M. Pertl, and M. Marinelli, "Grid frequency support by single-phase electric vehicles employing an innovative virtual inertia controller," in *Proc. IEEE 51st Int. Universities Power Eng. Conf.*, 2016, pp. 1–6.
- [16] S. Bruno, G. Giannoccaro, C. Iurlaro, M. La Scala, and C. Rodio, "Power hardware-in-the-loop test of a low-cost synthetic inertia controller for battery energy storage system," *Energies*, vol. 15, no. 9, 2022, Art. no. 3016. [Online]. Available: <https://www.mdpi.com/1996-1073/15/9/3016>
- [17] T.-T. Ku and C.-S. Li, "Implementation of battery energy storage system for an island microgrid with high PV penetration," *IEEE Trans. Ind. Appl.*, vol. 57, no. 4, pp. 3416–3424, Jul./Aug. 2021.
- [18] Y. Mitsugi, H. Hashiguchi, T. Shigemasa, Y. Ota, T. Terazono, and T. Nakajima, "Control hardware-in-the-loop simulation on fast frequency response of battery energy storage system equipped with advanced frequency detection algorithm," *IEEE Trans. Ind. Appl.*, vol. 57, no. 6, pp. 5541–5551, Nov./Dec. 2021.
- [19] D. Yao et al., "Frequency control ancillary service provided by a wind farm: Dual-BESS scheme," *J. Modern Power Syst. Clean Energy*, vol. 2, no. 2, pp. 93–103, Jun. 2014.
- [20] S. Bruno, G. De Carne, C. Iurlaro, C. Rodio, and M. Specchio, "A SOC-feedback control scheme for fast frequency support with hybrid battery/supercapacitor storage system," in *Proc. IEEE 6th Workshop Electron. Grid*, 2021, pp. 1–8.
- [21] F. Rubinstein, L. Xiaolei, and D. Watson, "Using dimmable lighting for regulation capacity and non-spinning reserves in the ancillary services market. A feasibility study," Lawrence Berkeley Nat. Lab., Berkeley, CA, USA, Tech. Rep. LBNL-4190E, 2010.
- [22] O. Ma et al., "Demand response for ancillary services," *IEEE Trans. Smart Grid*, vol. 4, no. 4, pp. 1988–1995, Dec. 2013.
- [23] M. Shahidepour, C. Bartucci, N. Patel, T. Hulsebosch, P. Burgess, and N. Buch, "Streetlights are getting smarter: Integrating an intelligent communications and control system to the current infrastructure," *IEEE Power Energy Mag.*, vol. 13, no. 3, pp. 67–80, May/Jun. 2015.
- [24] M. A. Ruiz, F. A. Abdallah, M. Gagnaire, and Y. Lascaux, "TeleWatt: An innovative electric vehicle charging infrastructure over public lighting systems," in *Proc. IEEE Int. Conf. Connected Veh. Expo.*, 2013, pp. 741–746.
- [25] S. Bruno, G. Giannoccaro, M. La Scala, G. Lopopolo, and C. Rodio, "A microgrid architecture for integrating EV charging system and public street lighting," in *Proc. IEEE Int. Conf. Environ. Elect. Eng. IEEE Ind. Commercial Power Syst. Europe*, 2019, pp. 1–5.
- [26] G. R. Newsham, S. Mancini, and R. G. Marchand, "Detection and acceptance of demand-responsive lighting in offices with and without daylight," *LEUKOS*, vol. 4, no. 3, pp. 139–156, 2008.
- [27] E. Waffenschmidt, "Virtual inertia grid control with LED lamp driver," in *Proc. IEEE Int. Energy Sustainability Conf.*, 2016, pp. 1–6.
- [28] M. Bagheri-Sanjareh, M. H. Nazari, and G. B. Gharehpetian, "A novel and optimal battery sizing procedure based on MG frequency security criterion using coordinated application of BESS, LED lighting loads, and photovoltaic systems," *IEEE Access*, vol. 8, pp. 95345–95359, 2020.

- [29] W. Wang, X. Chu, and K. Xiao, "A distributed economic AGC strategy integrating dynamic demand response," in *Proc. IEEE Power Energy Soc. Gen. Meeting*, 2018, pp. 1–5.
- [30] K. Xiao, X. Chu, and Y. Liu, "LED lighting loads actively participating in power system frequency regulation," in *Proc. IEEE Power Energy Soc. Innov. Smart Grid Technol. Conf.*, 2016, pp. 1–5.
- [31] J. Liu, W. Zhang, and Y. Liu, "Primary frequency response from the control of LED lighting loads in commercial buildings," *IEEE Trans. Smart Grid*, vol. 8, no. 6, pp. 2880–2889, Nov. 2017.
- [32] S. Bruno, G. Giannoccaro, C. Iurlaro, M. L. Scala, C. Rodio, and R. Sbrizzai, "Fast frequency regulation support by LED street lighting control," in *Proc. IEEE Int. Conf. Environ. Elect. Eng. IEEE Ind. Commercial Power Syst. Europe*, 2021, pp. 1–6.
- [33] M. G. Ippolito, R. Musca, E. R. Sanseverino, and G. Zizzo, "Frequency dynamics in fully non-synchronous electrical grids: A case study of an existing island," *Energies*, vol. 15, no. 6, 2022, Art. no. 2220.
- [34] M. L. Di Silvestre, D. La Cascia, E. Riva Sanseverino, and G. Zizzo, "Improving the energy efficiency of an islanded distribution network using classical and innovative computation methods," *Utilities Policy*, vol. 40, pp. 58–66, 2016.
- [35] UNI Technical Committee, "UNI 11248:2016 - Road lighting - Selection of lighting classes," pp. 1–38, 2016.
- [36] European Committee for Standardization, "EN 13201:2015 - road lighting - part 2: Performance requirements," 2015.
- [37] C. Cottarelli, C. Valdes, D. Bonata, F. Falchi, and R. Furgoni, "Illuminazione pubblica: Spendiamo troppo," Università del Sacro Cuore - Osservatorio CPI, Rome, Italy, Tech Rep., May 2018. [Online]. Available: https://osservatoriocpi.unicatt.it/cpi-17_Illuminazione_pubblica_21.05.18.pdf
- [38] Terna S.p.A., "Dati statistici sull'energia elettrica in Italia," Terna, Tech. Rep., 2017.
- [39] R. Eriksson, N. Modig, and K. Elkington, "Synthetic inertia versus fast frequency response: A definition," *IET Renewable Power Gener.*, vol. 12, no. 5, pp. 507–514, 2018.
- [40] S. Bruno, G. Giannoccaro, C. Iurlaro, M. L. Scala, and C. Rodio, "A low-cost controller to enable synthetic inertia response of distributed energy resources," in *Proc. IEEE Int. Conf. Environ. Elect. Eng. IEEE Ind. Commercial Power Syst. Europe*, 2020, pp. 1–6.
- [41] M. Rezkalla, A. Zecchino, S. Martinenas, A. M. Prostejovsky, and M. Marinelli, "Comparison between synthetic inertia and fast frequency containment control based on single phase EVs in a microgrid," *Appl. Energy*, vol. 210, pp. 764–775, 2018.
- [42] H. R. Chamorro et al., "Analysis of the gradual synthetic inertia control on low-inertia power systems," in *Proc. IEEE 29th Int. Symp. Ind. Electron.*, 2020, vol. 2020, pp. 816–820.



Sergio Bruno (Member, IEEE) received the master's and Ph.D. degree in electrical engineering from Politecnico di Bari, Bari, Italy, in 2000 and 2004, respectively. He has been involved as a Senior Scientist in several R&D project in the field of smart grids and energy systems. He is currently a tenure-track Associate Professor with Politecnico di Bari, where he holds the courses in power system automation and power quality, and manages the operational activities of the laboratory LabZERO. Since 2023, he has been the Vice-Chair of the IEEE Italy Section Chapter

PE31. His recent studies deal with power system automation, smart distribution systems, microgrids, energy services, and real-time simulation.



Giovanni Giannoccaro was born in Fasano, Italy, in 1980. He received the degree in electronic engineering with specialization in microelectronics from Politecnico di Bari, Bari, Italy, in 2011, and the Ph.D degree in electrical and information engineering on the topic energy saving and distributed microgeneration from Politecnico di Bari in 2016. In 2017, he was a Research Fellow on several industrial R&D projects. He is currently a Researcher in power systems with the Politecnico di Bari. His research interests include demand response, microgrid optimization and control, integration of energy infrastructures and innovation on devices, and services for energy utilization management.



Cosimo Iurlaro (Graduate Student Member, IEEE) was born in Taranto, Italy, in 1995. He received the degree (with Hons.) in electrical engineering with specialization in power system from the Polytechnic University of Bari, Bari, Italy, in 2019. He is currently working toward the Ph.D. degree in electrical and information engineering on the topic of power system. His research focuses on technologies and methodologies to provide energy services to the power system.



Massimo La Scala (Fellow, IEEE) is currently a Full Professor of electrical energy systems with Politecnico di Bari, Bari, Italy, and the Scientific Director of the Laboratory on Smart Grids and Energy Efficiency LabZERO. He is a Fellow Member of the IEEE and an active Researcher involved as Principal Investigator in numerous projects about smart grids and energy systems. He is with the Panel of Experts of the Italian Ministry of the University and Research in charge of issuing the Program of the Scientific Research for the period 2021–2027. He is with Consultative Group

to support the joint IEA-Italy Project: Smarter digital power infrastructure to enhance energy efficiency, resilient systems, and energy transition.



Marco Menga (Member, IEEE) was born in Martina Franca, Italy, in 1997. He received the master's degree (with Hons.) in electrical engineering from Politecnico di Bari, Bari, Italy, in 2021. Since 2021, he has been a Research Fellow in the field of electrical power systems with the Politecnico di Bari. His research interests include congestion management strategies and optimal dispatching of energy resources in electrical grids.



Carmine Rodio (Graduate Student Member, IEEE) was born in Cisternino, Italy, in 1986. He received the degree in electrical engineering from the Polytechnic University of Bari, Bari, Italy, in 2016. He is currently working toward the Ph.D. degree in electrical and information engineering in power system. His research interests include TSO-DSO coordination and market schemes to provide grid services by means of Distributed Energy Resources.



Roberto Sbrizzai received the degree in electrical engineering from the University of Bari, Bari, Italy, in 1986, and the Ph.D. degree in electrical engineering from the Politecnico di Bari, Bari, in 1992. He is currently an Associate Engineering Professor with the Electrical and Information Engineering Department, Politecnico di Bari. He is also a Lead Auditor for ISO certification of quality management systems. His research interests include planning, reliability, and optimization of electrical systems.